

NON-NORMAL AND NONLINEAR DYNAMICS OF THERMOACOUSTIC INSTABILITY IN A HORIZONTAL RIJKE TUBE

Sathesh Mariappan¹, R. I. Sujith^{*1}, Peter J. Schmid²

¹ Department of Aerospace Engineering, Indian Institute of Technology Madras
Chennai 600036, India

² Laboratoire d'Hydrodynamique (LadHyX), Ecole Polytechnique,
91128 Palaiseau cedex, France

* Corresponding author: sujith@iitm.ac.in

The paper focusses on the non-normal and nonlinear effects of thermoacoustic interaction in a horizontal electrically heated Rijke tube. The analysis starts with the governing equations for the fluid flow. The governing equations become stiff as the Mach number of the steady flow and the thickness of the heat source (compared to the acoustic wavelength) are small. Therefore asymptotic analysis is performed in the limit of small Mach number and compact heat source to eliminate the above stiffness problem. Two systems of governing equations are obtained: one for the acoustic field and the other for the unsteady flow field in the hydrodynamic zone around the heater. A theoretical framework is developed to understand the non-normal nature of the thermoacoustic interaction in the Rijke tube. The role of non-normality in the subcritical transition to instability regime is explored.

1 Introduction

Thermoacoustic instability is a plaguing problem in solid and liquid rockets, ramjets, aircraft and industrial gas turbines etc [13]. Thermoacoustic oscillations are sustained by the positive feedback of the unsteady heat release rate by the heat source (flame) in the combustion chamber to the chamber acoustic field. The problems due to thermoacoustic instability are identified only in the later stages of the development programme of aerospace vehicles. The complex interaction between the chamber acoustic field, the unsteady fluid flow and combustion makes the problem challenging. Thus, identifying instabilities in the early phase of the design stage is a formidable task. Thermoacoustic instability occurs, when the amplitude of acoustic pressure oscillations in the combustion chamber are amplified by the positive feedback of the unsteady heat release rate from the heat source in the chamber. Hence, understanding the coupling between the chamber acoustic field and the heat source is vital for the prediction and control of thermoacoustic instabilities. Towards this purpose, a mode of a Rijke tube with an electrical resistance heater as the heat source is analysed. Rijke tube is a simple thermoacoustic device, but has all the essential physics of thermoacoustic interaction. Rijke tube is an acoustic resonator tube, which consists of a heat source (in the present case, an electrical heater). The heat source is positioned at some axial location (Fig. 1). A mean flow is maintained at a desired flow rate using a blower.

Thermoacoustic instability of the Rijke tube has been studied for a long time. Acoustic oscillations in Rijke tube were first observed by Rijke [16] in a vertical tube with coiled electrical heating filament as the heat source. Self sustained thermoacoustic oscillations were observed when the

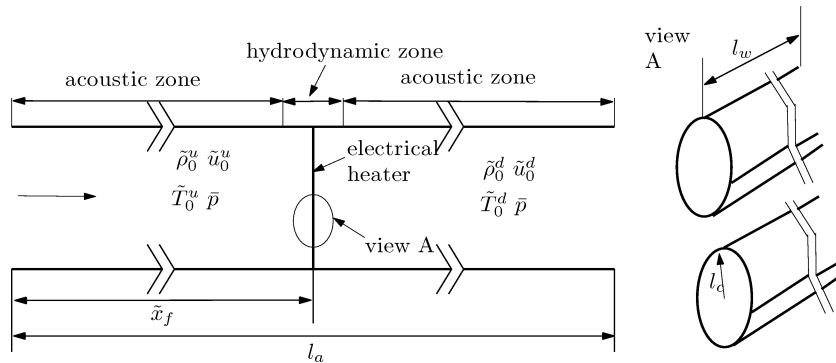


Figure 1: Configuration of the Rijke tube showing the acoustic and hydrodynamic zones

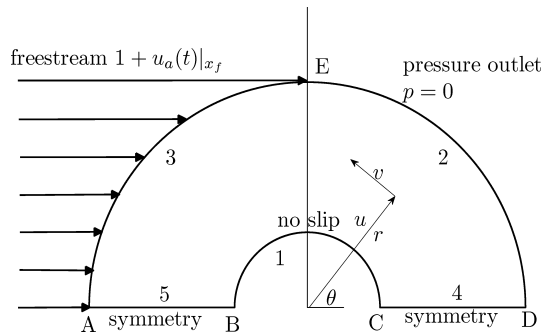


Figure 2: Flow domain and boundary conditions.

heater is positioned at some axial location of the tube and beyond some threshold power level. The reason is that thermoacoustic instability will occur if the unsteady heat release rate is in phase with the acoustic pressure oscillations [15]. This results in a positive feed back of energy from the heat source to the acoustic field, which increases the acoustic energy in the chamber. A number of numerical simulations [7, 9, 10] and experiments [12, 18] were performed to understand the basic mechanism of the coupling between the chamber acoustic field and the unsteady heat release rate. Numerical simulations were aimed to model the coupling between the chamber acoustic field and the unsteady heat release rate, to obtain the regions of stability of the system with the operating parameters and eventually design controller for the system. Two types of numerical approaches were taken in the past; time domain [9, 10] and frequency domain analysis [3, 8].

Till recently, investigations of thermoacoustic instability in Rijke tube system were focussed on the asymptotic state of the system (as $t \rightarrow \infty$). Thermoacoustic systems are shown to be non-normal, which leads to the non-orthogonality of eigenmodes [2]. This non-orthogonality of eigenmodes leads to transient growth of oscillations for appropriate set of initial conditions, even when the system is linearly stable. Hence it is important to investigate the short term dynamics of the system [11, 17]. The effects due to non-orthogonal eigenmodes in thermoacoustic systems were discussed in the context of thermoacoustic instability in ducted diffusion flame [1], Rijke tube [2] and solid rocket motor [11]. Farrell & Ioannou [4] have developed a generalised non-modal stability theory to analyse the linear stability of non-normal systems. He explained that the amount of transient growth depends on the choice of the initial condition. Hence it is important to find the initial condition ($t = 0$), which produces the maximum transient growth at a given time ($t = T_{opt}$). Conventional technique for obtaining the maximum transient growth and the corresponding initial condition is by performing singular value decomposition (SVD) on the linear operator governing the linearised system [4]. The above technique is suitable only for small systems (with small number of degrees of freedom). In the present paper, thermoacoustic instability in a

Rijke tube is investigated by simultaneously solving the governing equations for the acoustic field and the unsteady heat transfer from the heat source. In this manner, the dynamics associated with the heat source is also taken into account (previous investigation [11] shows the importance of the inclusion of the degrees of freedom associated with the dynamics of the heat source in the context of the non-normal nature of the system). Computational fluid dynamics technique is used to solve the equations, governing the dynamics of the heat source. Hence the number of grid points for numerically solving the governing equations is of the order 10^4 (see table 1), where the use of SVD to obtain the optimum initial condition for maximum transient growth becomes computationally costly.

In the present paper, another technique known as adjoint optimisation technique [6] is used to obtain the maximum transient growth and the corresponding initial condition for the linearised governing equations of thermoacoustic instability in the Rijke tube. Adjoint optimisation technique has been employed successfully in fluid mechanics [6].

The configuration of the Rijke tube investigated in the present paper is shown in Fig. 1. The following are the motivations for the present paper. 1). modeling the nonlinear nature of the thermoacoustic interaction in the Rijke tube, 2) investigation of the non-normal nature of thermoacoustic interaction in the Rijke tube, taking into account the dynamics of the heat source, 3) the third and the final motivation is to analyse the role played by non-normality in the subcritical transition regime of thermoacoustic instability.

2 Governing equations

The horizontal Rijke tube configuration considered here has a length l_a with the heater positioned at an axial location \tilde{x}_f (Fig. 1). The electrical resistance heater, which acts as a heat source is made up of a thin wire of radius l_c strung around the heater frame. The effective length of the wire filament, which participates in the heat transfer to the fluid flow is l_w . The typical length of the duct (l_a) is around $1m$ and the dimension of the heater along the axial direction of the tube (thickness, l_c) is around $1mm$. The zone around the heat source is termed as the hydrodynamic zone and its length in the axial direction of the Rijke tube is also of the order of the thickness of the heater. The thickness of the heater is very small compared to the length scale of the acoustic zone. Hence the heater and the hydrodynamic zone can be assumed to be compact compared to the acoustic zone in the tube. The acoustic and hydrodynamic zones are schematically shown in Fig. 1. The heater heats the flow and hence there is a temperature rise across the heater. Since the heater is compact, piecewise constant steady flow properties can be assumed on either side of the heater. The flow is at very low Mach number ($M \sim 10^{-3}$), which leads to a negligible steady state pressure loss. Hence the steady state pressure is assumed to be constant in space. All upstream steady state variables are known and specifying any one downstream steady state variable, such as temperature is enough to compute the other steady state variables from the following ideal gas and steady state continuity equations:

$$\tilde{\rho}_0^d = \frac{\tilde{\rho}_0^u \tilde{T}_0^u}{\tilde{T}_0^d}, \quad \tilde{u}_0^d = \frac{\tilde{\rho}_0^u \tilde{u}_0^u}{\tilde{\rho}_0^d} \quad (1)$$

where superscripts ‘ u ’ and ‘ d ’ represent upstream and downstream variables respectively, subscript ‘ 0 ’ represents steady variables and ‘ \sim ’ indicates dimensional variables. The non-dimensionalised governing equations are

$$\frac{\partial \rho}{\partial t_a} + M \nabla_a \bullet (\rho u) = 0 \quad (2a)$$

$$\rho \left(\frac{\partial}{\partial t_a} + M u \bullet \nabla_a \right) u + \frac{1}{\gamma M} \nabla_a p = \frac{M}{Re_a} \left(\nabla_a^2 + \frac{1}{3} \nabla_a (\nabla_a \bullet) \right) u \quad (2b)$$

$$\rho \left(\frac{\partial}{\partial t_a} + M u \bullet \nabla_a \right) T = \frac{\gamma - 1}{\gamma} \left(\frac{\partial}{\partial t_a} + M u \bullet \nabla_a \right) p + \frac{M}{Pe_a} \nabla_a^2 T \quad (2c)$$

where $Re_a = \bar{\rho}\bar{u}l_a/\mu$, $Pe_a = \bar{\rho}\bar{u}l_aC_p/k$, subscript ‘a’ indicates non-dimensionalisation performed with the acoustic length scale l_a . The non-dimensionalisation is performed as follows $\rho = \tilde{\rho}/\bar{\rho}$, $p = \tilde{p}/\bar{p}$, $u = \tilde{u}/\bar{u}$, $T = \tilde{T}/\bar{T}$, $x = \tilde{x}/l_a$, $t_a = \tilde{t}/(l_a/a)$, $t_c = \tilde{t}/(l_a/\bar{u})$, where $\bar{p} = \tilde{p}_0^u = \tilde{p}_0^d$, $\bar{\rho} = (\tilde{\rho}_0^u + \tilde{\rho}_0^d)/2$, $\bar{T} = \bar{p}/(\Re\bar{\rho})$, $\bar{u} = (\tilde{u}_0^u + \tilde{u}_0^d)/2$, $a = \sqrt{\gamma\Re\bar{T}}$, \Re is the specific gas constant and a is the local speed of sound.

Thermoacoustic instability analysis of the Rijke tube is the study of the dynamics of the coupled system comprising of the acoustic field in the tube and the unsteady heat transfer from the electrical wire filament. Therefore, it is important to track variations on the scale of the tube length (acoustic scale $l_a \sim 1m$) and on the scale of the heater wire filament radius ($l_c \sim 1mm$) in the hydrodynamic zone. Further, the acoustic time scale $t_{ac} = l_a/a$ and the wire heat transfer time scale $t_{cc} = l_c/\bar{U}$ are of the same order for typical values mentioned in the previous paragraphs. This leads to an effective coupling of the dynamics of the acoustic field and the unsteady heat release rate from the heater. The length and time scale ratios are defined as $\delta = l_c/l_a$, $\varepsilon = t_{ac}/t_{cc} = M/\delta \sim 1$. Now the present problem has two length scales separated by a large factor ($1/\delta \rightarrow \infty$) and one time scale ($\varepsilon \sim 1$). Asymptotic analysis has been performed on the governing equations and in the above limit ($\delta \rightarrow 0$, $M \rightarrow 0$, $\varepsilon \sim 1$), as the governing equations become stiff at low Mach numbers; in the present case $M \sim 10^{-3}$ [10]. A separate system of equations are obtained in the two zones; acoustic and hydrodynamic zone (see Fig. 1). The following ansatz for the flow variables is used as the initial step in the asymptotic analysis:

$$\begin{aligned} \rho &= \rho_s + M\rho_a, \quad u = u_s + u_a + u_c, \\ p &= 1 + Mp_a + M^2p_c, \quad T = T_s + T_c + MT_a \end{aligned} \quad (3)$$

where, subscript ‘s’ stands for steady state variables, ‘a’ for fluctuations due to acoustic field, ‘c’ for fluctuations in the hydrodynamic zone. Here, acoustic fluctuations exist all along the length of the tube, while the fluctuations due to heater exists in a zone around the heater (hydrodynamic zone), which is small compared to the acoustic length scale. Hence the variables with subscript ‘a’ exist over the length of the tube (acoustic zone, see Fig. 1), while the variables with subscript ‘c’ exists over the region around the heater wire filament length scale l_c (hydrodynamic zone, see Fig. 1) and vanishes as one moves away from the heater. The explanation for choosing the particular form (power series in M) of the above ansatz (3), the detailed derivation of obtaining the separate equations for the two zones (acoustic and hydrodynamic zones) and the coupling between them are given in [10]. Only the final system of governing equations are shown in the present paper. There are two separate system of equations; one in the acoustic zone and another in the hydrodynamic zone. A brief description of the system of equations is presented. The system of equations in the acoustic zone (one dimensionalised along the length of the Rijke tube) is as follows:

$$\rho_s \frac{\partial u_a}{\partial t_a} + \frac{1}{\gamma} \frac{\partial p_a}{\partial x_a} = 0 \quad (4a)$$

$$\frac{1}{\gamma} \frac{\partial p_a}{\partial t_a} + \frac{\partial u_a}{\partial x_a} + \zeta_n \omega_n p_a = q \widehat{\delta}(x - x_f) \quad (4b)$$

where $\zeta_n = (C_1(\omega_n/\omega_1) + C_2\sqrt{\omega_1/\omega_n})/(2\pi)$, ζ_n represents damping in the acoustic zone due to viscosity and end losses, C_1 , C_2 are the coefficients which determine the amount of damping [12] and $\omega_n/2\pi$ is the frequency associated with the Galerkin basis function (see § 4.1 of [10]) of the oscillation, $\widehat{\delta}(x)$ is the Dirac-delta function, which is used to include the compactness of the hydrodynamic zone in the acoustic equations, subscript ‘a’, ‘q’ is obtained from (5) and $\partial/\partial x_a$ represents derivatives in the acoustic length scale l_a . The above system of equations (4) are solved by Galerkin technique as described in [10]. Similarly the system of equations in the hydrodynamic zone is as follows:

$$\nabla_c \bullet (u_p) = 0 \quad (5a)$$

$$\left(\frac{\partial}{\partial t_c} + u_p \bullet \nabla_c \right) u_p + \frac{1}{\gamma} \nabla_c p_c = \frac{1}{Re_c} \nabla_c^2 u_p + \frac{\partial u_a}{\partial t_c} \Big|_{x_f} \quad (5b)$$

$$\frac{\partial T_p}{\partial t_c} + u_p \bullet \nabla_c T_p = \frac{1}{Pe_c} \nabla_c^2 T_p \quad (5c)$$

where, $q = \frac{l_w l_c}{Pe_c S_c} \left[\left(\int_0^{2\pi} \nabla_c \left((\tilde{T}_w - \tilde{T}_0^u) T_p / \bar{T} - T_s \right)_{\hat{e}_r} d\theta \right) \right]$, $t_c = \varepsilon t_a$, $u_p = u_a|_{x_f} + u_s + u_c$, $u_a|_{x_f}$ represents acoustic velocity (u_a) at the non-dimensional heater location x_f , $\partial u_a / \partial t_c|_{x_f}$ represents $\partial u_a / \partial t_c$ at x_f , $Re_c = \bar{\rho} \bar{u} l_c / \mu$, $Pe_c = \bar{\rho} \bar{u} l_c C_p / k$, S_c represents the cross section area of the Rijke tube and ∇_c represents gradient in the length scale of the hydrodynamic zone l_c . One of the aims of the present paper is to obtain the optimum initial condition for maximum growth of perturbations at any given time T_{opt} . Hence, a brief explanation about non-normal operator and its connection to the present system of equations (4 & 5) are given in the following section.

3 Non-normality and transient growth

A linear dynamical system ($d\chi/dt = L\chi$) is said to be non-normal if the linear operator ‘ L ’ governing the evolution of the system does not commute with its adjoint L^\dagger ($LL^\dagger \neq L^\dagger L$, \dagger indicates adjoint operator) [5]. In such systems, the eigenmodes (eigenvectors) are non-orthogonal. Any initial condition for the system can be written as a linear combination of the eigenmodes. For a linearised system, stable under classical linear stability (all the eigenvalues lie in the left half of the complex plane), all the eigenmodes are decaying monotonically in time. However, in the case of non-normal system, the vectorial sum of the eigenmodes which gives the state of the system at any time ‘ t ’ can increase (for suitable initial condition) for a short time and eventually decay after a long time [1, 17]. Mathematically a transient growth occurs in the evolution of the L_2 norm of the system ($\|\chi\|^2 = \chi^\dagger \chi$), which can be related to a physical energy in the disturbance [11, 17]. The interplay between non-normality (transient growth) and nonlinearity plays an important role in the subcritical transition to instability [1, 11].

In order to study the non-normal nature of the present Rijke tube system, the system of equations (4, 5) are linearised, to obtain the linear operator ‘ L ’. The linear operator L thus obtained does not commute with its adjoint. The system of equations in the acoustic zone (4) is shown to be non-normal due to the inclusion of the unsteady heat release term ‘ q ’ by [2]. Also the equation (5b) is nothing but the Navier-Stokes equation for incompressible flows, with an additional global acceleration term $\partial u_a / \partial t_c|_{x_f}$. The Navier-Stokes equation is shown to be non-normal. Hence the coupled system of equations (4 & 5) is non-normal. The amount of transient growth to be obtained in a non-normal system depends on the initial condition. As the first step in the optimisation procedure, the governing equations (5 & 4) (also called as direct equations) with the corresponding boundary conditions are written in the appropriate domain as explained in the following section.

4 Direct equations

This section deals with the direct equations governing the thermoacoustic instability in a Rijke tube. Since the heater coil in its primitive form is a cylinder (Fig. 1), the system of equations (5) is solved for the configuration of flow over an heated cylinder. A two dimensional flow over cylinder is considered, as the spacing between the heating wire filament is very large compared to the wire diameter (wire diameter $\sim mm$, coil diameter $\sim cm$). Due to the absence of vortex shedding (see Appendix of [10]) phenomenon, only one-half of the flow field is simulated and the symmetry boundary condition is enforced. Plane polar coordinate ($u_p = (u_p)\hat{e}_r + (v_p)\hat{e}_\theta$) system is used so as to implement the no-slip boundary condition on the surface of the wire filament (circular cylinder). Moreover, fluid viscosity and thermal conductivity are assumed to be independent of temperature so that momentum and energy equations are decoupled.

Linear optimal is obtained in the present investigation; i.e. the optimum initial condition obtained from the linearised governing equations. The present paper applies the adjoint optimisation procedure to a problem which involves two length scale problems. Obtaining nonlinear optimal; i.e., the optimal initial condition obtained from the nonlinear governing equations is beyond the scope of the present paper. It is recommended to first obtain the linear optimal and study the evolution of the linear optimal and understand the role of non-normality on the dynamics of the system. Obtaining the nonlinear optimal can be performed as the next step. In obtaining the linear optimal, the governing equations (4, 5) are linearised with the following decomposition $(u_p)\hat{e}_r = \bar{U} + u'$, $(v_p)\hat{e}_\theta = \bar{V} + v'$, $p_p = \bar{P} + p'$, $T_p = \bar{T} + T'$, where over bar ($\bar{\quad}$) indicates the steady state variables and prime ($'$) indicates the fluctuations from the steady state. The linearised governing equations are as follows (primes $'$ are removed for convenience):

$$F_1 = \rho_s \frac{\partial u_a}{\partial t_a} + \frac{1}{\gamma} \frac{\partial p_a}{\partial x_a} = 0 \quad (6a)$$

$$F_2 = \frac{1}{\gamma} \frac{\partial p_a}{\partial t_a} + \frac{\partial u_a}{\partial x_a} + \zeta_n \omega_n p_a - \left(k \int_0^\pi \frac{\partial T}{\partial r} \Big|_{(1,\theta,t_a)} d\theta \right) \delta(x - x_f) = 0 \quad (6b)$$

$$F_3 = \frac{\partial u}{\partial r} + \frac{u}{r} + \frac{1}{r} \frac{\partial v}{\partial \theta} = 0 \quad (6c)$$

$$F_4 = \frac{\partial u}{\partial t_c} + 2 \frac{\partial (\bar{U}u)}{\partial r} + \frac{1}{r} \frac{\partial (\bar{U}v + \bar{V}u)}{\partial \theta} + \frac{2}{r} (\bar{U}u - \bar{V}v) + \frac{\partial p}{\partial r} - \frac{1}{Re} \left(\nabla^2 u - \frac{u}{r^2} - \frac{2}{r^2} \frac{\partial v}{\partial \theta} \right) - \frac{\partial u_{af}}{\partial t} \cos \theta = 0 \quad (6d)$$

$$F_5 = \frac{\partial v}{\partial t_c} + \frac{\partial (\bar{U}v + \bar{V}u)}{\partial r} + \frac{2}{r} \frac{\partial (\bar{V}v)}{\partial \theta} + \frac{2}{r} (\bar{U}v + \bar{V}u) + \frac{1}{r} \frac{\partial p}{\partial \theta} - \frac{1}{Re} \left(\nabla^2 v + \frac{2}{r^2} \frac{\partial u}{\partial \theta} - \frac{v}{r^2} \right) + \frac{\partial u_{af}}{\partial t} \sin \theta = 0 \quad (6e)$$

$$F_6 = \frac{\partial T}{\partial t_c} + \bar{U} \frac{\partial T}{\partial r} + u \frac{\partial \bar{T}}{\partial r} + \frac{\bar{V}}{r} \frac{\partial T}{\partial \theta} + \frac{v}{r} \frac{\partial \bar{T}}{\partial \theta} - \frac{1}{Pe} \nabla^2 T = 0 \quad (6f)$$

where, $k = 2l_w l_c (\tilde{T}_w - \tilde{T}_0^u) / (Pe_c S_c \bar{T})$, \tilde{T}_w is the surface temperature of the heater wire, \tilde{T}_0^u is the temperature upstream of the heater. The boundary conditions corresponding to eqns. (6) are the following:

Acoustic zone:

$$H_{a_1} = p_a(0, t) - p_{a0} = 0 \quad (7a)$$

$$H_{a_2} = p_a(1, t) - p_{a1} = 0 \quad (7b)$$

Hydrodynamic zone:

In the hydrodynamic zone, the numerical subscript indicates the location of the boundary condition as in Fig. (2), whereas the last subscript represents the variable to which the boundary condition is applied. For eg., H_{h1_u} has the numerical subscript '1', which corresponds to the surface of the cylinder as shown in Fig. 2 and the last subscript 'u' represents the variable u .

$$H_{h1_u} = u(1, \theta, t) - u_0 = 0, \quad 0 \leq \theta \leq \pi \quad (8a)$$

$$H_{h2_u} = \partial u(\infty, \theta, t) / \partial r - u_{\infty d} = 0, \quad 0 \leq \theta \leq \pi/2 \quad (8b)$$

$$H_{h3_u} = u(\infty, \theta, t) - u_{af} \cos \theta = 0, \quad \pi/2 < \theta \leq \pi \quad (8c)$$

$$H_{h4_u} = \partial u(r, 0, t) / \partial \theta - u_{s1} = 0, \quad 1 \leq r < \infty \quad (8d)$$

$$H_{h5_u} = \partial u(r, \pi, t) / \partial \theta - u_{s2} = 0, \quad 1 \leq r < \infty \quad (8e)$$

$$H_{h1_v} = v(1, \theta, t) - v_0 = 0, \quad 0 \leq \theta \leq \pi \quad (9a)$$

$$H_{h2_v} = \partial v(\infty, \theta, t) / \partial r - v_{\infty d} = 0, \quad 0 \leq \theta \leq \pi/2 \quad (9b)$$

$$H_{h3_v} = v(\infty, \theta, t) + u_{af} \sin \theta = 0, \quad \pi/2 < \theta \leq \pi \quad (9c)$$

$$H_{h4_v} = v(r, 0, t) - v_{s1} = 0, \quad 1 \leq r < \infty \quad (9d)$$

$$H_{h5_v} = v(r, \pi, t) - v_{s2} = 0, \quad 1 \leq r < \infty \quad (9e)$$

$$H_{h1_p} = \partial p(1, \theta, t) / \partial r - p_{0d} = 0, \quad 0 \leq \theta \leq \pi \quad (10a)$$

$$H_{h2_p} = p(\infty, \theta, t) - p_\infty = 0, \quad 0 \leq \theta \leq \pi/2 \quad (10b)$$

$$H_{h3_p} = \partial p(\infty, \theta, t) / \partial r - p_{\infty d} = 0, \quad \pi/2 < \theta \leq \pi \quad (10c)$$

$$H_{h4_p} = \partial p(r, 0, t) / \partial \theta - p_{s1} = 0, \quad 1 \leq r < \infty \quad (10d)$$

$$H_{h5_p} = \partial p(r, \pi, t) / \partial \theta - p_{s2} = 0, \quad 1 \leq r < \infty \quad (10e)$$

$$H_{h1_T} = T(1, \theta, t) - T_0 = 0, \quad 0 \leq \theta \leq \pi \quad (11a)$$

$$H_{h2_T} = \partial T(\infty, \theta, t) / \partial r - T_{\infty d} = 0, \quad 0 \leq \theta \leq \pi/2 \quad (11b)$$

$$H_{h3_T} = T(\infty, \theta, t) - T_\infty = 0, \quad \pi/2 < \theta \leq \pi \quad (11c)$$

$$H_{h4_T} = \partial T(r, 0, t) / \partial \theta - T_{s1} = 0, \quad 1 \leq r < \infty \quad (11d)$$

$$H_{h5_T} = \partial T(r, \pi, t) / \partial \theta - T_{s2} = 0, \quad 1 \leq r < \infty \quad (11e)$$

The initial conditions for (6) are given by

$$G_{u_a} = u_a(x, 0) - u_a^0 = 0 \quad (12a)$$

$$G_{p_a} = p_a(x, 0) - p_a^0 = 0 \quad (12b)$$

$$G_u = u(r, \theta, 0) - u^0 = 0 \quad (12c)$$

$$G_v = v(r, \theta, 0) - v^0 = 0 \quad (12d)$$

$$G_p = p(r, \theta, 0) - p^0 = 0 \quad (12e)$$

$$G_T = T(r, \theta, 0) - T^0 = 0 \quad (12f)$$

where $p_{a0} = p_{a1} = u_0 = u_{\infty d} = u_{s1} = u_{s2} = \dots = T_{s1} = T_{s2} = 0$. Having obtained the linearised governing equations for the Rijke tube system, the next step is to define an energy, which measures the growth or decay of disturbances.

5 Myers' energy

Disturbance energy is defined as the energy stored in any perturbations and can be used as a measure of growth or decay of the perturbations in a dynamical system. The starting point for the derivation of generalized disturbance energy is the expression from [14], who obtained energy in any arbitrary perturbations with mean flow taken into account. The perturbations are not restricted to an acoustic disturbance. They can be any generalised perturbations in the flow field. In the present paper, the disturbance energy corresponding to the second order energy corollary from [14] is used, as the asymptotic expansion (eq. 3) has terms upto second order in M . The

Table 1: Physical parameters in acoustic zone, hydrodynamic zone and convergence parameters in for solving the direct and adjoint equations

acoustic zone	hydrodynamic zone	convergence parameters		
$l_a = 1 \text{ m}, S_c = 0.01 \text{ m}^2$	$Re_d = 20,$	hydrodynamic zone grids $(r, \theta) = 100 \times 120$		
$\bar{P} = 1 \text{ bar}$	$l_c = 1 \text{ mm}$	residue	direct	adjoint
$\tilde{\rho}_0^u = 1.025 \text{ kg m}^{-3}$	$l_w = 16.4 \text{ m}$	continuity	10^{-5}	10^{-2}
$\tilde{T}_0^u = 295 \text{ K}$	$\tilde{T}_w = 1000 \text{ K}$	momentum	10^{-5}	10^{-5}
$\tilde{T}_0^d = 500 \text{ K}$	$M = 5 \times 10^{-4}$	energy	10^{-5}	10^{-5}

disturbance energy per unit volume (\tilde{E}_v), as defined by [14] for (eq. 2) is

$$\tilde{E}_v = \frac{\bar{\rho}\bar{U}^2}{2} \left(\frac{\bar{P}}{\bar{\rho}\bar{U}^2} \left(\left(\frac{\rho'}{\rho_s} \right)^2 + \frac{1}{\gamma-1} \left(\frac{T'}{T_s} \right)^2 \right) + \rho_s u'^2 + 2u_s \rho' u' \right) \quad (13)$$

where prime (') represents the fluctuating quantities from the steady state. The fluctuating quantities in the above equation are identified from the ansatz (eq. 3) as following:

$$\begin{aligned} \rho' &= M\rho_a, \quad u' = u_a + u_c, \\ p' &= Mp_a + M^2p_c, \quad T' = T_c + MT_a \end{aligned} \quad (14)$$

The total disturbance energy (\tilde{E}_d) is the integral of \tilde{E}_v over the entire volume. The total non-dimensionalised disturbance energy, $E_d = \tilde{E}_d/(\bar{\rho}\bar{u}^2 S_c l_a/2)$ and is given by:

$$\begin{aligned} E_d = E_{ac} + E_c &= \underbrace{\int_0^{x_f-\varsigma} \left(\left(\frac{p_a}{\gamma} \right)^2 + \rho_s u_a^2 \right) dx_a + \int_{x_f+\varsigma}^1 \left(\left(\frac{p_a}{\gamma} \right)^2 + \rho_s u_a^2 \right) dx_a}_{\text{acoustic zone}} \\ &+ \underbrace{\frac{2l_w l_c^2}{S_c l_a} \int_{r=1}^{\infty} \int_{\theta=0}^{\pi} \lambda(r) (u^2 + v^2) r dr d\theta + \frac{2l_w l_c^2 (\tilde{T}_w - \tilde{T}_0^u)}{S_c l_a \gamma M (\gamma - 1) \bar{T}} \int_{r=1}^{\infty} \int_{\theta=0}^{\pi} \frac{T^2}{T_s} r dr d\theta, \quad \varsigma \rightarrow 0}_{\text{hydrodynamic zone}} \end{aligned} \quad (15)$$

where $\lambda(r) = e^{-((r-1)/l_{cu})^2}$ is used for the convergence of the integral [6], l_{cu} is the cut-off radius. The disturbance energy (E_d) obtained is also used as a measure for examining the growth or decay of oscillations in the system. The above expression for disturbance energy (eq. 15) is used as the norm to study the non-normal nature of the present Rijke tube system. This norm is used in the cost functional, which is to be maximised over all possible initial conditions and is taken up in the following section.

6 Definition of the cost functional and adjoint equations

As already explained in § 3, thermoacoustic systems are non-normal. Due to the non-normal nature, the system shows a transient growth in energy during the evolution of an initial perturbation, even for a linearly stable system. But eventually the oscillations decay to zero. This transient growth must be measured with some scalar measure. The last section § 4 dealt with the energy to be used to analyse the non-normal nature of the present thermoacoustic system. At the present level, amplification of energy (from $t = 0$) stored in a small arbitrary perturbation (Myers' energy, § 5) is used as the measure for quantifying transient growth. The cost functional (\mathfrak{J} , eq. 16) is defined

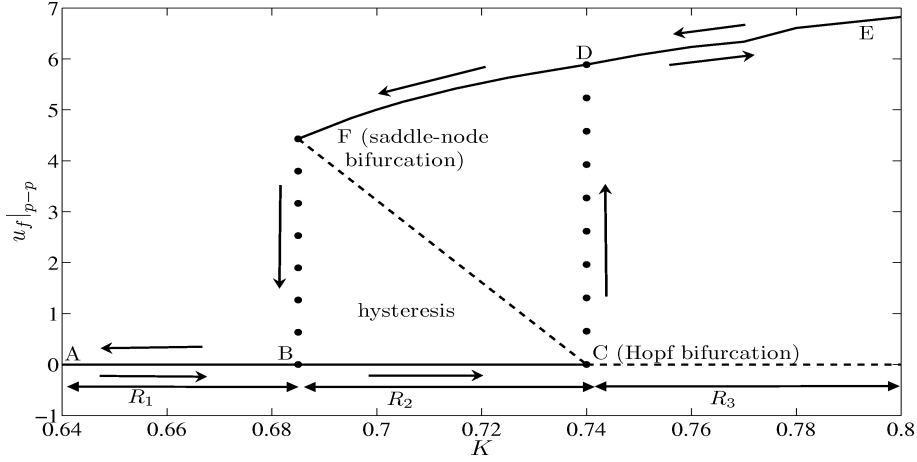


Figure 3: Bifurcation diagram with non-dimensional heater power ‘ K ’ as the control parameter. The other parameters are, $C_1 = 0.3$, $C_2 = 0.1$, $x_f = 0.25$. Various regimes are R_1 - linearly and nonlinearly stable, R_2 - linearly stable, but nonlinearly unstable and R_3 - linearly and nonlinearly unstable.

as the ratio of E_d^t at time $t = T$ and $t = 0$.

$$\mathfrak{S} = \frac{E_d^{T_{opt}}(p_a, u_a, u, v, p, T)}{E_d^0(p_a, u_a, u, v, p, T)} \quad (16)$$

Adjoint optimisation technique is used to obtain the optimum initial condition, which maximises \mathfrak{S} at $t = T_{opt}$ over all possible initial conditions. The optimisation technique can be found in [6].

7 Results and discussion

Numerical simulations are performed with the parameters shown in table (1). Unless specified, the parameter values in table (1) are used for the simulations.

7.1 Asymptotic stability

Figure 3 shows the bifurcation diagram for thermoacoustic instability of the Rijke tube system with the non-dimensional heater power K as the control parameter. In the vertical axis, the peak to peak value of acoustic velocity ($u_f|_{p-p}$) (obtained by the difference between the maximum and minimum values of u_f during the asymptotic state of the system) at the heater location (x_f) in the asymptotic time limit is marked. This serves as a measure of the asymptotic state of the system. Solid lines indicate stable solutions, while broken lines indicates unstable solutions in the asymptotic time limit. For low values of the K (say $K = 0.66$), there is only one asymptotic state ($u_f = 0$) and that is the stable fixed point (stable focus).

As the heater power is increased, beyond $K = 0.685$, two stable solutions exist: 1) stable focus to which all the trajectories nearby spiral into it, 2) stable limit cycle, where finite amplitude oscillation occur in the asymptotic time limit. The first one (stable focus) shows that the system is linearly stable; i.e. stable to small amplitude perturbations. However, for large perturbation amplitudes, the system reaches the second solution (limit cycle). There is a critical initial condition, which demarcates the above two dynamical behaviours. This represents the basin boundary (line CF, indicated qualitatively) of the two attractors (stable focus and limit cycle), whose shape is complicated as the degrees of freedom of the system considered is very large. Thus the system, which is stable to small amplitude perturbations, becomes unstable and eventually reaches a limit

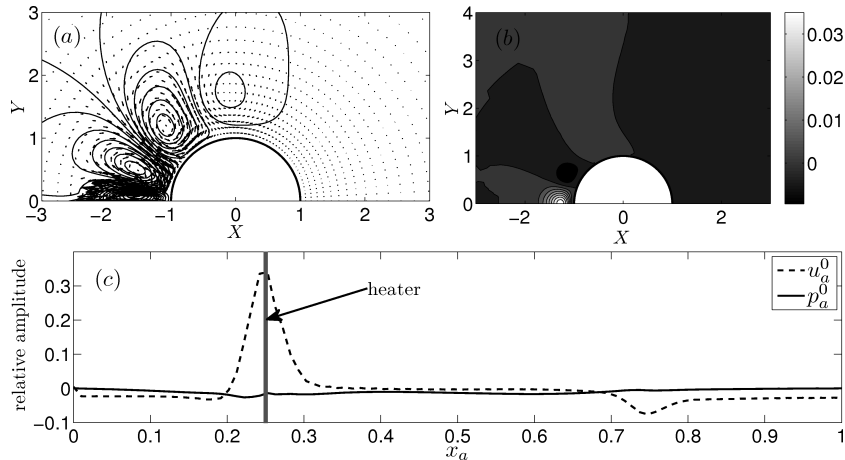


Figure 4: Distribution of optimum initial condition in the state space variables $C_1 = 0.3$, $C_2 = 0.1$, $x_f = 0.25$, $K = 0.735$, $\alpha = 3.3 \times 10^{-3}$, $\beta = 3.77 \times 10^4$, $T_{opt} = 0.5$, $L_{cu} = 35$, (a) streamlines and velocity vectors corresponding to u & v , (b) temperature field T in the hydrodynamic zone, (c) acoustic field in the acoustic zone.

cycle for large amplitude perturbations. In the same figure, the dotted line represents the unstable limit cycle. They are not obtained from numerical simulations and are shown only to indicate a typical basin boundary qualitatively. Now, further increasing K beyond point C ($K = 0.74$) results in linearly unstable system, where the system is unstable to small amplitude perturbations also. Only one stable solution exists, which is the limit cycle. Also the limit cycle amplitude increases as the heater power is increased. Thus bifurcation diagram shows the complete regimes of asymptotic stability for the Rijke tube system for variation of the system parameters. From the bifurcation diagram, one can observe that the region R_2 is the region where subcritical transition to instability occurs.

7.2 Short time behaviour of the system

The last section dealt with the asymptotic stability of the system. The effects of the non-normal nature of the Rijke tube system appears in the initial short time evolution of the system. The following sections deals with the structure of the optimum initial condition and its effect on the asymptotic stability of the system in the subcritical transition regime ($k = 0.738$, see Fig. 3).

7.2.1 Optimum initial condition

The distribution of the optimum initial condition in the state space variables is shown in Fig. (4). One can observe in the flow field corresponding to u & v , distinct patches of vortical structures are present (Fig. 4a). The temperature (T) contours (Fig. 4b) also shows a similar distinct patches as that of the flow field. The initial acoustic velocity (u_a^0) distribution shows a peak at the location of the heater. In the present paper, Galerkin technique is used to solve the acoustic equations (eq. 4). In order to capture the Dirac-delta function, which is used to represent the compactness of the heat source (eq. 6b), a total of 100 Galerkin modes are used and a corresponding modal convergence (less than 5 % change in the spatial variation of u_a & p_a) has been achieved for the optimum initial condition in the acoustic zone.

7.2.2 Role of non-normality in subcritical transition to instability

The present subsection discusses the role of non-normal effects on the evolution of the system. The evolution of the system from various kinds of initial conditions are analysed. In this section, two

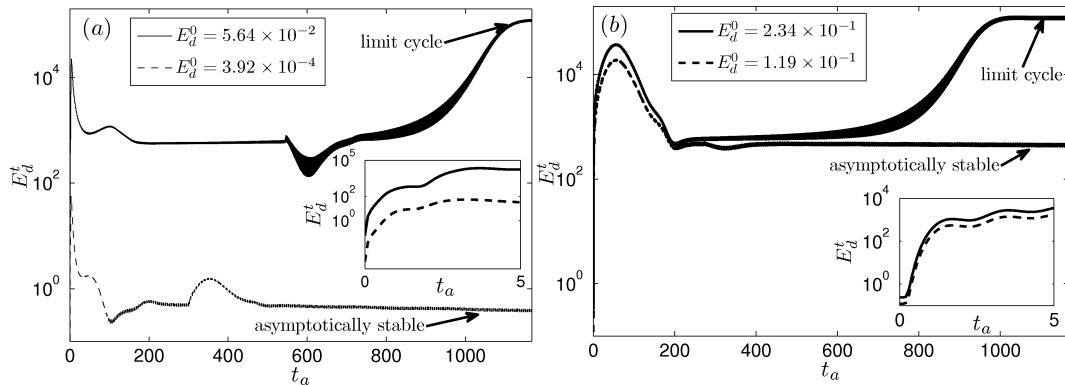


Figure 5: Comparison of the evolution of the disturbance energy E_d^t with the initial condition, a) optimum initial condition ($T_{opt} = 0.5$, Fig. 4) and b) acoustic initial condition ($u_a^0(x_a) = A \cos(\pi x_a)$, $p_a^0(x_a) = u^0 = v^0 = T^0 = 0$, ‘A’ determines the initial energy of the disturbance) having different initial energy (the inset shows evolution of E_d^t zoomed near the initial evolution). $C_1 = 0.3$, $C_2 = 0.05$, $K = 0.738$.

kinds of initial conditions are investigated. The first one is the optimum initial condition (see Fig. 4) for maximum transient growth in \mathfrak{S} and the second kind is the acoustic initial condition, where fundamental natural duct mode of the system is excited initially. In Fig. 5, the evolution of E_d^t for various strengths of the optimum and acoustic condition are shown. Figure 5a, shows the system with $E_d^0 = 5.64 \times 10^{-2}$ reaches a limit cycle with the optimum initial condition. The system is stable for energies lesser than $E_d^0 = 5.64 \times 10^{-2}$ in the optimum initial condition (obtained from the numerical simulations from a time marching code). On the other hand, Fig. 5b indicates that the system reaches a limit cycle for $E_d^0 = 2.34 \times 10^{-1}$ for an acoustic initial condition. The initial energy for the acoustic initial condition ($E_d^0 = 2.34 \times 10^{-1}$) is an order of magnitude more than the initial energy for the optimum initial condition ($E_d^0 = 5.64 \times 10^{-2}$) for the system to be nonlinearly unstable and reach a limit cycle. For the present simulation, the linear stability theory predicts that the system is stable. The prediction fails, when the initial condition is above some threshold energy. This threshold energy varies for the two kinds of initial conditions discussed. The threshold energy is less (by an order of magnitude) for the optimum initial condition compared to the acoustic initial condition. Hence the non-normal nature of the system is reflected in the reduction in the range of linearisation (threshold energy) of the system.

8 Conclusion

Thermoacoustic instability analysis of a horizontal electrically heated Rijke tube is performed. The analysis started with an examination of the conservation equations for fluid flow. In the limit of zero Mach number and compact size of the heat source compared to the acoustic length scale, the equations become stiff. Hence asymptotic analysis is performed, which gave further physical insight into the problem. Two separate system of equations are obtained: one for the acoustic zone and the other for the hydrodynamic zone. The separation into two systems of equations occurred in an elegant way and the coupling between the two appeared naturally. In analysing the non-normal nature of the system, the optimum initial condition obtained has contributions both in the acoustic and the hydrodynamic zone. In the hydrodynamic zone, optimum initial condition projects as distinct patches of high vorticity and corresponding patches in the temperature field. The threshold energy for the system to reach a limit cycle is shown to be less for the optimum initial condition than for the acoustic initial condition.

The authors thank IITM for providing access to the High Performance Computing Environment

(HPCE) for the present study, the financial support from Department of Science and Technology (DST), India and Ecole Polytechnique, France. The authors also thank Prof. W. Polifke, TU München and Dr. M. P. Juniper, University of Cambridge for the fruitful discussions with them during the initial formulation of the problem.

References

- [1] K. Balasubramanian and R. I. Sujith. Non-normality and nonlinearity in combustion acoustic interaction in diffusion flames. *Journal of Fluid Mechanics*, 594:29–57, 2008.
- [2] K. Balasubramanian and R. I. Sujith. Thermoacoustic instability in a Rijke tube: Non-normality and nonlinearity. *Phy. Fluids*, 20:044103, 2008.
- [3] S. Bittanti, A.D. Marco, G. Poncia, and W. Prandoni. Identification of a model for thermoacoustic instabilities in a Rijke tube. *IEEE Transactions on control systems technology*, 10:490–502, 2002.
- [4] B. F. Farrell and P. J. Ioannou. Generalized stability theory. part i. autonomous operators. *Journal of the Atmospheric Sciences*, 53(14):2025–2040, 1996.
- [5] G. H. Golub and C. E. Van Loan. *Matrix Computations*. The Johns Hopkins University Press, UK, 1989.
- [6] A. Guegan, P. J. Schmid, and P. Huerre. Spatial optimal disturbances in swept attachment-line boundary layers. *Journal of Fluid Mechanics*, 603:179–188, 2008.
- [7] C. C. Hantschk and D. Vortmeyer. Numerical simulation of self-excited thermoacoustic instabilities in a Rijke tube. *Journal of Sound and Vibration*, 227:511–522, 1999.
- [8] M. A. Heckl and M. S. Howe. Stability analysis of the Rijke tube with a Green’s function approach. *Journal of Sound and Vibration*, 305:672–688, 2007.
- [9] Y. P. Kwon and B. H. Lee. Stability of the Rijke thermoacoustic oscillation. *J. Acoust. Soc. Am.*, 78:1414–1420, 1985.
- [10] S. Mariappan and R. I. Sujith. Modeling nonlinear thermoacoustic instability in an electrically heated rijke tube. *48th AIAA Aerospace Sciences Meeting Including the New Horizons Forum and Aerospace Exposition, 4 - 7 January 2010, Orlando, Florida, AIAA 2010-25*, 2010.
- [11] S. Mariappan and R. I. Sujith. Thermoacoustic instability in solid rocket motor - non-normality and nonlinear instabilities. *accepted for publication in J. Fluid Mech.*, 2010.
- [12] K. I. Matveev. *Thermo-acoustic instabilities in the Rijke tube: Experiments and modeling*. PhD thesis, California Institute of Technology, Pasadena, 2003.
- [13] K. Mcmanus, T. Poinsot, and S. Candel. A review of active control of combustion instabilities. *Progress in Energy and Combustion Science*, 19:1 – 29, 1993.
- [14] M. K. Myers. Transport of energy by disturbances in arbitrary steady flows. *J. Fluid Mech.*, 226:383–400, 1991.
- [15] L. Rayleigh. The explanation of certain acoustical phenomenon. *Nature*, 18:319–321, 1878.
- [16] P. L. Rijke. The vibration of the air in a tube open at both ends. *Philosophical Magazine*, 17:419–422, 1859.
- [17] P. J. Schmid and D. S. Henningson. *Stability and Transition in Shear Flows*. Springer-Verlag, New York, 2001.
- [18] W. S. Song, S. Lee, D. S. Shin, and Y. Na. Thermo-acoustic instability in the horizontal Rijke tube. *Journal of Mechanical Science and Technology*, 20:905–913, 2006.